Applied Catalysis B: Environmental 191 (2016) 228–234

Contents lists available at ScienceDirect

Applied Catalysis B: Environmental

journal homepage: www.elsevier.com/locate/apcatb

In-situ synthesis and enhanced photocatalytic activity of visible-light-driven plasmonic Ag/AgCl/$NaTaO_3$ nanocubes photocatalysts

Dongbo Xu[a,b], Weidong Shi[a,b,*], Chengjie Song[c], Min Chen[b], Songbo Yang[b], Weiqiang Fan[b], Biyi Chen[b]

[a] School of Energy and Power Engineering, Jiangsu University, Zhenjiang 212013, PR China
[b] School of Chemistry and Chemical Engineering, Jiangsu University, Zhenjiang 212013, PR China
[c] School of Environmental and Safety Engineering, Changzhou University, Changzhou 213164, PR China

ARTICLE INFO

Article history:
Received 29 December 2015
Received in revised form 14 March 2016
Accepted 15 March 2016
Available online 16 March 2016

Keywords:
Ag/AgCl/$NaTaO_3$
Photocatalyst
Plasmon
Visible light
Dye degradation

ABSTRACT

In this paper, the novel plasmonic Ag/AgCl/$NaTaO_3$ photocatalysts were prepared by a precipitation and photoreduction method then studied the photocatalytic properties. The crystal structure of the photocatalysts was characterized by X-ray diffraction and the morphology and composition were studied by scanning electron microscopy, transmission electron microscopy, X-ray photoelectron spectroscopy and energy-dispersive X-ray. The transmission electron microscopy shows that the Ag ions were finally formed on the surface of AgCl by in situ photoreaction. The photocatalytic examination of the photocatalysts was carried out through the decomposition methylene blue, rhodamine-B and phenol aqueous solution under visible-light irradiation. Compared to the pure $NaTaO_3$ nanocubes and Ag/AgCl nanoparticles, the Ag/AgCl/$NaTaO_3$ photocatalysts show superior photocatalytic activities and still had good photocatalytic activity after five cycles. The UV–vis diffuse reflectance, photoluminescence and photo-electrochemical measurement of the Ag/AgCl/$NaTaO_3$ photocatalysts verified that the enhancing photocatalytic activity was resulted from the ability for absorbing visible-light and the electron-hole pair high separation. Additionally, based on the active species trapping and electron spin resonance experiments, the photocatalytic mechanism was proposed over Ag/AgCl/$NaTaO_3$ photocatalysts for organics degradation.

1. Introduction

It is well-known that environmental pollution has become the critical issues around the world. Especially, the industry and modern society have a huge development in the present century. A number of organic pollutants are discharged into the water [1,2]. So far, the photocatalysts have attracted extensive interest for solving waste water by using sunlight [3–5]. Simultaneously, the visible-light-driven photocatalysts have attracted much attention because the sunlight was consisted of visible light about 50%, but the ultraviolet light (UV) was only about 4%. From the extensive research, plasmonic composites photocatalysts based on Ag/AgCl display higher photocatalytic performance for dye degradation than single-component ones [6–8]. For example, Chen et al. [9] reported a Ag@AgCl nanotubes fabricated from copper nanowires. Habibi-Yangjeh et al. [10] prepared a Ag/AgCl sensitized ZnO nanostructures plasmonic photocatalyst by one-pot ultrasonic-assisted method. Wang et al. [11] through ion-exchange treatment and light-induced reduction process synthesized Ag@Ag(Br, I) photocatalyst. With Ag/AgCl as plasmonic photocatalysts, the surface plasmon resonance (SPR) of Ag nanoparticles (NPs) have a great absorption under the visible light irradiation. Subsequently, the Ag/AgCl and semiconductor have a strong interaction on the surface of semiconductor so that can speed up the separation of electrons and holes, then enhanced the photocatalytic activities. Recently, Ag/AgCl/semiconductor photocatalysts have been synthesized and they have high photocatalytic activities under visible light have been reported [12–15].

In recent years, tantalates as functional materials are widely used in photochemical and photocatalysis because of their appropriate semiconducting nature. The conduction bands of tantalates

* Corresponding author at: School of Energy and Power Engineering, Jiangsu University, Zhenjiang 212013, PR China.
E-mail addresses: swd1978@ujs.edu.cn, shiwd999@yahoo.com (W. Shi).

http://dx.doi.org/10.1016/j.apcatb.2016.03.036
0926-3373/

are consisting of Ta5d orbital which are more negative position compared to the niobates (Nb4d) and titanates (Ti3d) orbital. Therefore, the tantalates photocatalysts are very good for water splitting and organic pollutants degradation in water. Such as alkali tantalates $LiTaO_3$, $NaTaO_3$, and $KTaO_3$ as well as alkaline earth tantalates $SrTa_2O_6$, $CaTa_2O_6$, $BaTa_2O_6$ [16–20]. However, these tantalates are only photoexcited under UV light. With the Ag/AgCl properties, it is an enormous untapped potential to enhance the photocatalytic activity of tantalates for preparing the new composites by using Ag/AgCl.

Herein, we report a facile process for preparation plasmonic Ag/AgCl/$NaTaO_3$ photocatalysts. For the first, the $NaTaO_3$ nanocubes were synthetized by hydrothermal method. As the second, the AgCl NPs via a precipitation method were deposited on the surface of $NaTaO_3$ nanocubes. Finally, through photoreduction reaction the Ag/AgCl/$NaTaO_3$ photocatalysts were successfully prepared. The photocatalytic activity of Ag/AgCl/$NaTaO_3$ photocatalysts were evaluated by degrading MB and RhB under visible light irradiation. The degradation mechanism of Ag/AgCl/$NaTaO_3$ photocatalysts was discussed.

2. Experimental

2.1. Preparation

All of the reagents were analytical grade and used without further purification. $NaTaO_3$ nanocubes were synthesized by the reported hydrothermal method [21]. Typically, the $NaTaO_3$ nanocubes and 25 mL distilled water were added in a 50 mL beaker and vigorous stirring at room temperature. Then a certain amount of $AgNO_3$ aqueous solution was added in the beaker and finally added excessive amounts of HCl aqueous solution under magnetic stirring for 2 h. The AgCl NPs were synthesized and deposited on the surface of the $NaTaO_3$ nanocubes. The as-prepared photocatalysts were irradiated under a 300 W xenon lamp for 20 min so that the partial Ag^+ ions from AgCl were reduced to Ag° species. The resulting photocatalysts were washed by distilled water and ethanol same times until the pH 7.0 and the final products were dried at 60 °C for 24 h. For comparison, Ag/AgCl photocatalysts were prepared by excessive amounts of HCl aqueous solution added to the $AgNO_3$ aqueous solution.

2.2. Characterization

The crystal structures were characterized by a Bruker D8 diffractometer using the Cu-Kα radiation source at a scan rate (2θ) of 7°/s. The morphologies and composition of the photocatalysts were examined with S-4800 field emission scanning electron microscope (SEM, Hitachi, Japan) equipped with an energy-dispersive X-ray spectroscope (EDS). Transmission electron microscopy (TEM) and high resolution transmission electron microscopy (HRTEM) analyses were conducted with a JEM-2100F electron microscope (JEOL, Japan). X-ray photoelectron spectroscopy (XPS) analysis were performed with a VG ESCALAB 250 XPS system with Al Kα X-ray source (1253.6 eV) source. All of the binding energies were referenced to the C1s peak at 284.8 eV of the surface adventitious carbon. UV–vis diffuse reflectance spectra (DRS) were recorded on a UV–vis spectrophotometer (Shimadzu UV-3100, Japan) using $BaSO_4$ as a reference standard. Steady state luminescence (PL) experiments were performed using a Photon Technology International Model Quantamaster-QM4m spectrofluorimeter equipped with a 75 W lamp and dual excitation monochromators. The photocurrent was measured with an electrochemical analyzer (CHI 660B Chenhua Instrument Company). The electron spin resonance (ESR) analysis was conducted with an electron paramagnetic resonance spectrometer (A300-10/12, Bruker).

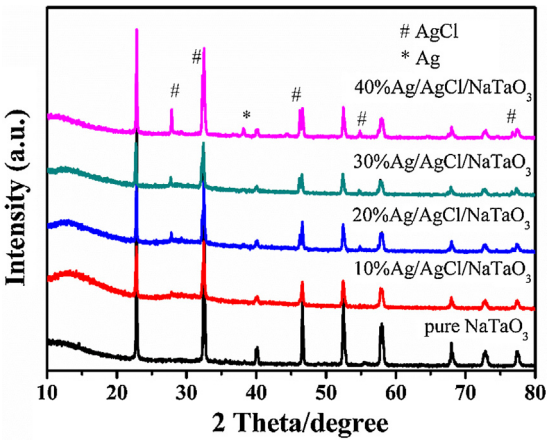

Fig. 1. XRD patterns of pure $NaTaO_3$ and Ag/AgCl/$NaTaO_3$ photocatalysts.

2.3. Photocatalytic activity

The photocatalytic activity of the Ag/AgCl/$NaTaO_3$ photocatalysts was evaluated by the degradation of MB and RhB aqueous solution because they are chemically stable and persistent dye pollutant. Experiments were carried out in a home-built reactor with a water jacket so that by circulating water through the jacket the experiments were kept at constant temperature. 0.1 g photocatalysts were placed in a 100 mL MB, RhB and phenol aqueous solution (10 mg/L) in the reactor, respectively. Prior to irradiation, the suspensions was magnetically stirred for 30 min to reach an adsorption-desorption equilibrium in the dark. A 250 W Xe lamp with a UV-cutoff filter (>425 nm) was used as a visible light source to trigger the photocatalytic reaction. Every 10 min, 5.0 mL of solution was taken out and centrifuged then sent to UV–vis absorption measurement.

2.4. Photoelectrochemical measurements

To investigate the photocatalysts photoelectrochemical properties, the photocurrents were measured on an electrochemical analyzer in a standard three-electrode system using the prepared photocatalysts dropped onto a piece of FTO slice as the working electrodes, a Pt wire as the counter electrode, and Ag/AgCl (saturated KCl) as a reference electrode. A 50 W Xe arc lamp served as a light source. The photocurrent was performed in sodium sulfate solution (Na_2SO_4, 0.5 M, pH 7.0).

3. Results and discussion

3.1. Materials characterization

The typical XRD patterns of the synthesized Ag/AgCl/$NaTaO_3$ photocatalysts with different compositions are shown in Fig. 1. The diffractions of pure $NaTaO_3$ correspond to the JCPDS card No. 25-0863. However, with the weight percent of Ag/AgCl added, at the first, the AgCl phases (JCPDS No. 31-1238) was found and the peaks were marked with "#". When the weight percent of Ag/AgCl was sequentially added, the peaks marked with "*" are assigned to the phases of Ag (JCPDS No. 04-0783). In the XRD spectrum, the characteristic diffraction peaks at 46.2° and 57.5° correspond to the (2 2 0) and (2 2 2) crystal planes of AgCl. As shown in Fig. 1, the weak peaks at 38.2° suggest that the small quantity of Ag phases with the plane (3 1 1) was formed in the Ag/AgCl/$NaTaO_3$ photocatalysts. The XRD

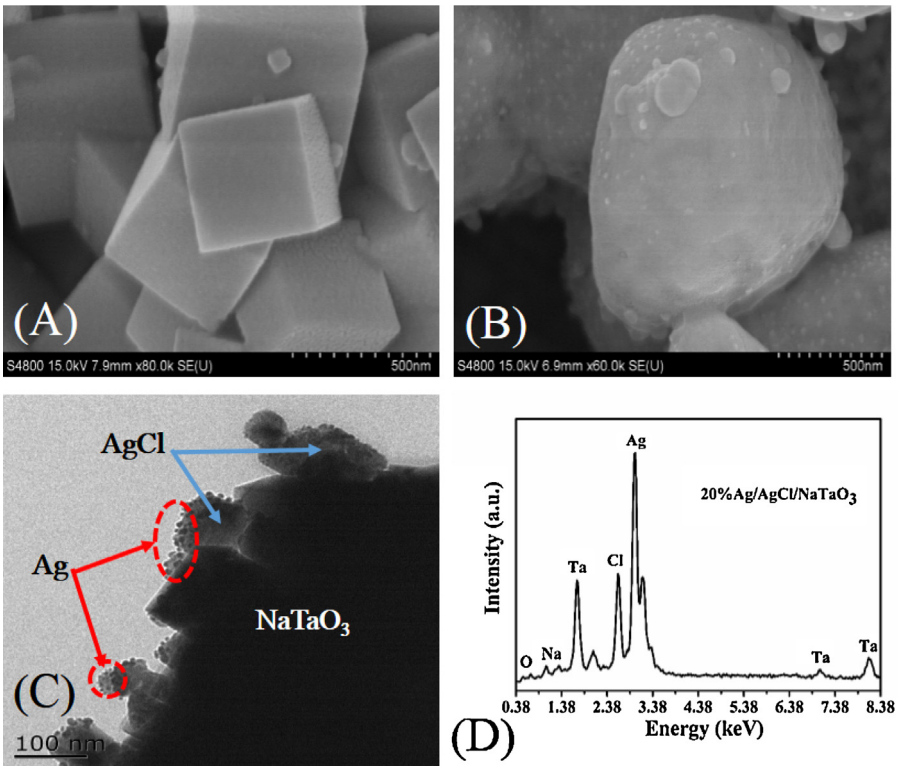

Fig. 2. SEM images of (A) $NaTaO_3$ and (B) Ag/AgCl, (C) TEM image of 30% Ag/AgCl/$NaTaO_3$ and (D) the EDS spectra of 20%Ag/AgCl/$NaTaO_3$.

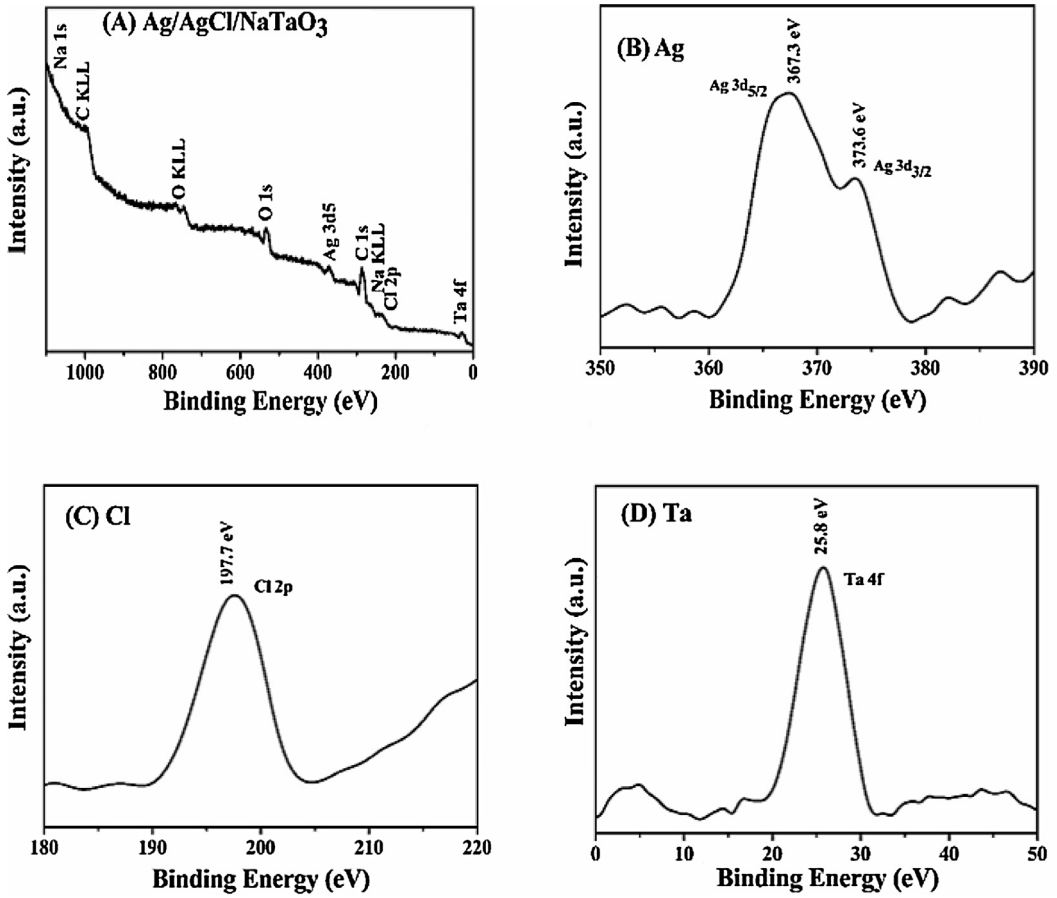

Fig. 3. XPS survey spectrum (A) and XPS spectra of Ag (B), Cl (C) and Ta (D) of the as-prepared 30% Ag/AgCl/$NaTaO_3$ photocatalysts.

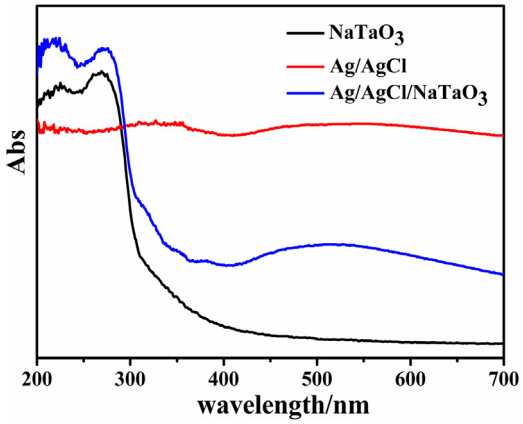

Fig. 4. UV–vis diffuse reflectance spectra of pure $NaTaO_3$, Ag/AgCl and 30% $Ag/AgCl/NaTaO_3$ photocatalysts.

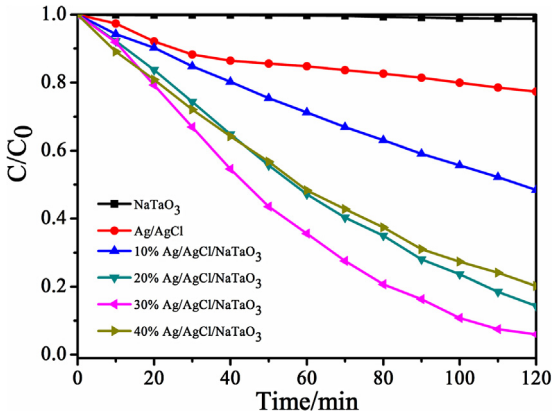

Fig. 5. Comparison of various photocatalysts degradation of RhB with the same weight.

results indicated that the Ag/AgCl NPs should be only deposited on the surface of $NaTaO_3$ nanocubes and no other diffraction peaks were detected in the patterns.

Typical morphology of the prepared $NaTaO_3$ photocatalysts was characterized by the SEM as shown in Fig. 2A. It is clear to see that the $NaTaO_3$ was compose of nanocubes. Fig. 2B was the typical SEM images of the as-obtained Ag/AgCl NPs. It is clearly observed that the AgCl are heterogeneous particles and it can be seen that there are Ag NPs attached on the surface of AgCl particles. Interestingly, as shown in Fig. 2C, the TEM image of 30% $Ag/AgCl/NaTaO_3$ plasmonic photocatalysts show that the photocatalysts are composed of $NaTaO_3$ nanocubes, AgCl and Ag NPs and the Ag ions are obvious on the surface of AgCl. Such an $Ag/AgCl/NaTaO_3$ nanostructure can fully use the $NaTaO_3$ nanocubes outer surface so that it is beneficial for enhance the photocatalytic activity on degradation of organic dye pollutants. To determine the composition of $Ag/AgCl/NaTaO_3$ photocatalysts, the corresponding EDS spectra are measured. As shown in Fig. 2D, it can be seen that there are strong signals from Ag and Cl, Ta, O, Na. Such a result indicates that the $Ag/AgCl/NaTaO_3$ photocatalysts is consisted of Ag, Cl, Ta, O and Na elements. Compared to the XRD result, it is clearly that the $Ag/AgCl/NaTaO_3$ photocatalysts have been synthesized successfully. The HRTEM image of 30% $Ag/AgCl/NaTaO_3$ (Fig. S2) shows the clear lattice fringes of the Ag and AgCl NPs. The interplanar spacing of 0.20 nm and 0.16 nm are consistent with the (2 2 0) and (2 2 2) crystal face of AgCl, respectively. The interplanar spacing of 0.12 nm is consistent with the (3 1 1) crystal face of Ag. The result of HRTEM is in good agreement with the XRD results.

In order to determine the elemental composition and the chemical status of the $Ag/AgCl/NaTaO_3$ photocatalysts, the XPS was measured. As shown in Fig. 3A, the XPS survey spectrum, it can be seen that the signals from elements of Ta, Ag, Cl, O and C. The Ag spectrum in Fig. 3B displays two peaks at 367.3 and 373.6 eV, which could be assigned to Ag $3d_{5/2}$ and Ag $3d_{3/2}$ from AgCl [22–25], respectively. Meanwhile, the peak at 367.3 eV was divided into another peak at 367.4 eV and the peak at 373.6 eV was as well as divided into another peak at 373.5 eV. (Fig. S1, Supporting information) However, these two peaks can be correspond to the Ag° because the spin energy separation was 6.1 eV according to the reports [26,27]. As shown in Fig. 3C and D, the peaks at 197.7 eV and 25.8 eV could be assigned to the Cl 2p and Ta 4f, respectively [28–30]. The observations of XPS results which are consistent with the XRD further confirm that a content of metallic Ag° was obtained.

Light absorption properties of pure $NaTaO_3$, Ag/AgCl and 30% $Ag/AgCl/NaTaO_3$ photocatalysts are compared in Fig. 4. The properties are very important in degradation of dyes pollutants for their application. From Fig. 4, the Ag/AgCl is able to absorb visible-light irradiation. In contrast to the pure $NaTaO_3$, the 30% $Ag/AgCl/NaTaO_3$ photocatalysts have a strong adsorption peak (from 442 to 700 nm) by the Ag/AgCl surface plasmon resonance observed in the visible region. The $Ag/AgCl/NaTaO_3$ photocatalysts have a strong absorption under visible light irradiation suggests that it can efficiently utilize the visible light for the degradation of organic dyes pollutants.

3.2. Photocatalytic activity

As shown in Fig. 5, the photocatalytic activity of $Ag/AgCl/NaTaO_3$ photocatalysts for degradation of RhB molecules under visible light irradiation was displayed. From the degradation results, the pure $NaTaO_3$ only slightly degraded the RhB under visible light. The test confirmed that the degradation was negligible. However, the $Ag/AgCl/NaTaO_3$ photocatalysts exhibited good photocatalytic activity under identical experimental conditions. After 2 h irradiation, the Ag/AgCl degraded RhB only about 20%. The 10% $Ag/AgCl/NaTaO_3$ and 20% $Ag/AgCl/NaTaO_3$ photocatalysts degraded nearly 50% and 85% of RhB after 2 h irradiation, respectively. The highest photocatalytic activity was the 30% $Ag/AgCl/NaTaO_3$ photocatalysts that at the same time an approximate 92% of RhB was degraded. In addition, the 40% $Ag/AgCl/NaTaO_3$ photocatalysts have more weight percent of Ag/AgCl then the 30% $Ag/AgCl/NaTaO_3$ photocatalysts but the photocatalytic activity are lower. The reason is that when the Ag/AgCl over the limit value, much too Ag/AgCl on the surface of $NaTaO_3$ which lead to less h^+ and e^- generation and lower h^+ and e^- separation efficiency so that the photocatalytic activity decreased. According to the results, indicating that the Ag/AgCl modified the $NaTaO_3$ have a significantly improved the photocatalytic activity for the degradation of RhB and the excellent photocatalytic activities of $Ag/AgCl/NaTaO_3$ photocatalysts are thanks to be the surface plasmon resonance of Ag/AgCl and the interaction between Ag/AgCl and $NaTaO_3$ [31].

MB is another typical dye pollutant that without absorption in the visible light region so that was selected to degradation. As shown in Fig. 6, the absorbance of MB was evaluated with irradiation time on the $Ag/AgCl/NaTaO_3$ photocatalysts. From Fig. 6, we can see that the MB photodegradation of pure $NaTaO_3$ under visible light can be negligible. However, nearly 99% of MB has been degraded with the 30% $Ag/AgCl/NaTaO_3$ photocatalysts. The Fig. 6 results are as the same with Fig. 5 indicate that the $Ag/AgCl/NaTaO_3$ are good photocatalysts for degradation organic dyes pollutant under visible light. In order to avoid dye self-sensitized in the photocatalytic decomposition process, another colorless organic compound of phenol was chosen to evaluate the photocatalytic activity of $Ag/AgCl/NaTaO_3$ photocatalysts. As shown in Fig. S3,

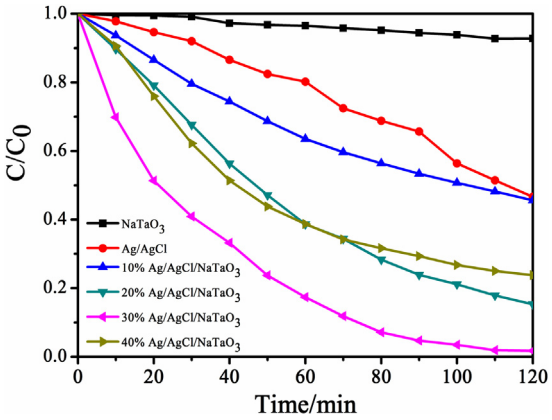

Fig. 6. Comparison of various photocatalysts degradation of MB.

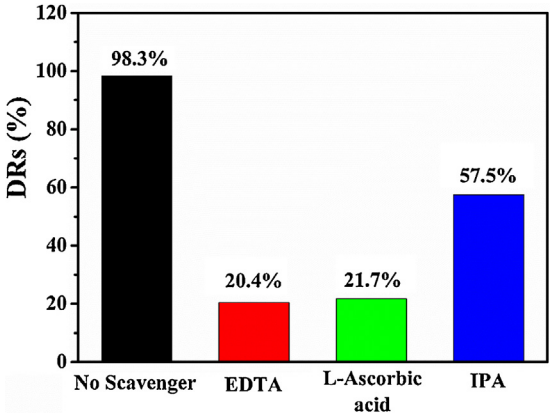

Fig. 8. The degradation of MB on the 30% Ag/AgCl/$NaTaO_3$ photocatalysts in presence of various scavengers.

the experimental results obtained indicated that the phenol degradation rates were 1%, 28% and 50% over pure $NaTaO_3$, Ag/AgCl and Ag/AgCl/$NaTaO_3$ under visible light irradiation, respectively. By comparison of the phenol degradation rates, the photocatalytic activity of Ag/AgCl/$NaTaO_3$ was confirmed for the degradation of phenol. The reusability is very important for the photocatalysts with the real application. In order to study the reusability of the Ag/AgCl/$NaTaO_3$ photocatalysts, the photocatalytic degradation experiments of RhB and MB were repeated five times. As shown in Fig. 7, after five-cycle tests of RhB and MB photodecomposition, the photocatalytic activity of the photocatalysts is no obvious loss. Hence, these results strongly indicate that the photocatalysts are good for reusability under visible light irradiation.

To investigate the reactive species of Ag/AgCl/$NaTaO_3$ photocatalysts in the photocatalytic mechanism, a series of scavengers was used during the degradation of MB photochemical reaction process. Fig. 8 shows the results in the presence of the selected scavengers. In this study, EDTA was scavenger of holes (h^+), L-ascorbic acid was added as a superoxide ions ($^\bullet O_2^-$) scavenger, and iso-propyl alcohol (IPA) was used as a hydroxyl radical ($^\bullet$OH) scavenger, respectively [32–34]. It is evident that no scavengers the degradation rate is 98.3%. However, in the presence of EDTA and L-ascorbic acid, the decrease of the rate are similar to each other, 20.4% and 21.7%, respectively. When in the presence of IPA, the degradation rate is 57.5%. Based on these results, it can be concluded that the h^+ and $^\bullet O_2^-$ are the important role and the $^\bullet$OH plays acted a secondary role in the photocatalytic degradation. However, in this study, considering that the Cl^- could be oxidized by h^+ to Cl°, the organic dye could be decreased by the Cl° [35–37]. It was thought that the Cl° was another actual active specie in the photocatalytic degradation process.

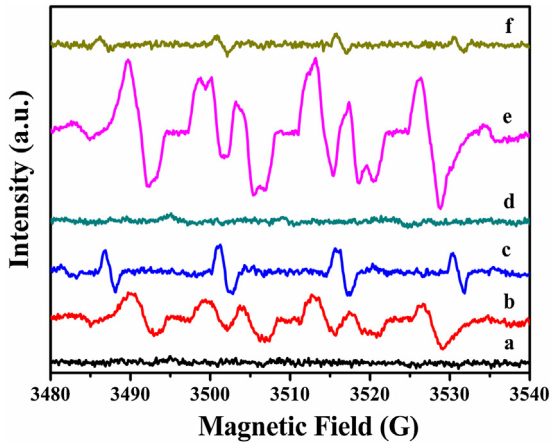

Fig. 9. ESR spectra of radical adducts trapped by DMPO for prepared photocatalysts: (a) Ag/AgCl-DMPO in dark; (b) Ag/AgCl-DMPO-$^\bullet O_2^-$ and (c) Ag/AgCl-DMPO-$^\bullet$OH formed under light irradiation; (d) 30% Ag/AgCl/$NaTaO_3$-DMPO in dark; (e) 30% Ag/AgCl/$NaTaO_3$-DMPO-$^\bullet O_2^-$ and (f) 30% Ag/AgCl/$NaTaO_3$-DMPO-$^\bullet$OH formed under light irradiation.

To clarify the photocatalytic mechanism, the ESR technique was used to explore the reactive species. As shown in Fig. 9, there is no ESR signals in the dark for Ag/AgCl and 30% Ag/AgCl/$NaTaO_3$ photocatalysts, but a gradual signals for $^\bullet O_2^-$ and $^\bullet$OH of Ag/AgCl photocatalysts are observed under light irradiation and the characteristic peaks are similar to the previous studies for $^\bullet O_2^-$ and $^\bullet$OH adduct [38]. Note that the characteristic peaks of $^\bullet O_2^-$ and $^\bullet$OH are equal altitude. It indicate that in Ag/AgCl system for degradation,

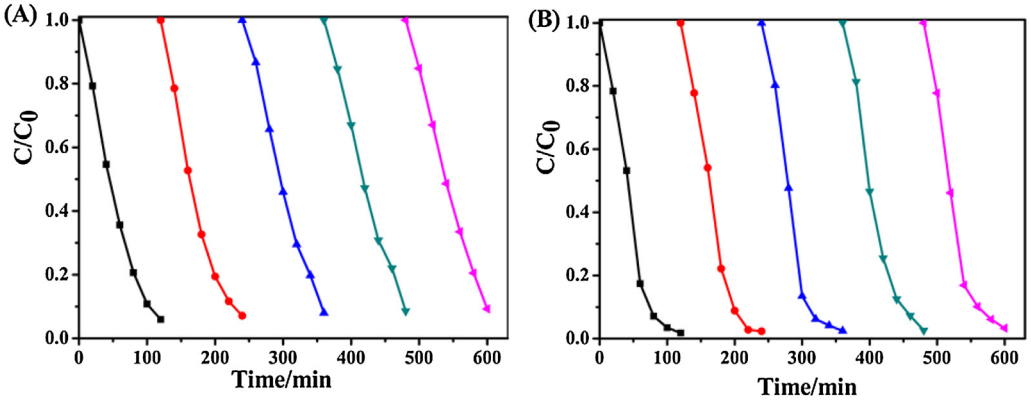

Fig. 7. Cycling runs for photocatalytic degradation of RhB (A) and MB (B) over the 30% Ag/AgCl/$NaTaO_3$ photocatalysts under visible light irradiation.

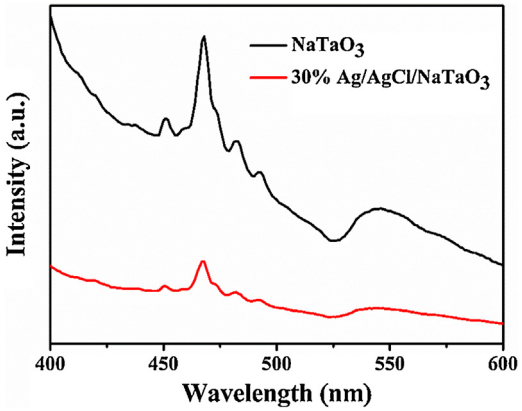

Fig. 10. Schematic diagram for the charge separation in a visible light irradiated Ag/AgCl/$NaTaO_3$ system.

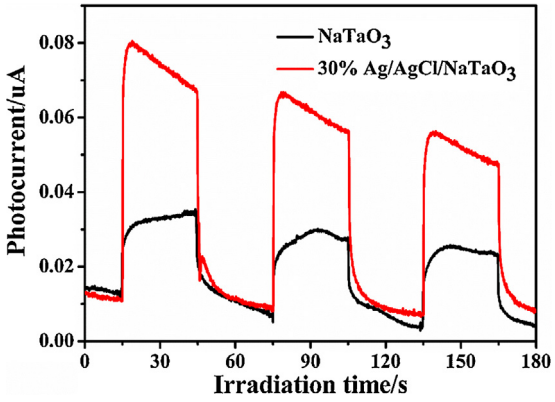

Fig. 11. Transient photocurrent response for the pure $NaTaO_3$ and the 30% Ag/AgCl/$NaTaO_3$ photocatalysts.

the $^{\bullet}O_2^-$ and •OH act as the predominant species. Similarly, there are the obvious signals of $^{\bullet}O_2^-$ and •OH in 30% Ag/AgCl/$NaTaO_3$ system under light irradiation. Compared to the Ag/AgCl system, the peaks of $^{\bullet}O_2^-$ are stronger and the peaks of •OH are weaker in the 30% Ag/AgCl/$NaTaO_3$ system. The ESR results confirm that the $^{\bullet}O_2^-$ radicals exist in the Ag/AgCl/$NaTaO_3$ system which is the principal active specie for the photodegradation of organic dyes. The ESR results are consistent with the active species trapping experiment.

The photoluminescence (PL) spectra were used to confirm the photogenerated electrons (e^-) and h^+ recombination efficiency. The higher recombination probability of photogenerated charges will display higher intensity in the PL spectra [39]. The PL spectra of $NaTaO_3$ nanocubes and Ag/AgCl/$NaTaO_3$ photocatalysts are presented in Fig. 10, at the wavelength of 472 nm emission. The Ag/AgCl/$NaTaO_3$ photocatalysts displays lower PL intensity than pure $NaTaO_3$ nanocubes, which means the Ag/AgCl/$NaTaO_3$ photocatalysts have a higher separation efficiency of the photoexcited e^- and h^+. Therefore, the SPR of Ag/AgCl on the surface of $NaTaO_3$ could contribute to improve the separation efficiency of photoexcited e^- and h^+ in the Ag/AgCl/$NaTaO_3$ photodegradation system and hence, the plasmon Ag/AgCl/$NaTaO_3$ have a higher photocatalytic activity.

It is known that the photocurrent can supply an evidence to support that the separation efficiency of e^- and h^+ in the photocatalytic reaction [40]. The higher photocurrents are indicative of better e^- and h^+ separation and higher photocatalytic activity [41]. Then the transient photocurrent responses of pure $NaTaO_3$ and 30% Ag/AgCl/$NaTaO_3$ photocatalysts were tested and showed 3 cycles of light irradiation on-off in Fig. 11. It is clear that Ag/AgCl/$NaTaO_3$ photocatalysts show much higher photocurrent density than that of pure $NaTaO_3$, which means the more efficient separation of the photoinduced e^- and h^+. The result of the photocurrents analysis was consistent with the PL analysis, which further confirmed the Ag/AgCl has been effectively combined with the $NaTaO_3$ and enhanced photoinduced charge carrier separation efficiency with the higher interfacial charge transfer rate on the surface of $NaTaO_3$.

Based on the above results, the photocatalytic reaction of Ag/AgCl/$NaTaO_3$ can be understood by the following mechanism as similar to the plasmon-induced charge separation and Ag/AgCl plasmonic photocatalysis which are reported by Tatsuma and Huang, respectively [42,43]. In the Ag/AgCl system, the Ag NPs absorbed the photon on the visible region then was separated into e^- and h^+ such that the e^- transferred to the surface of Ag NPs then was trapped by O_2 to form $^{\bullet}O_2^-$ species. Meanwhile, half of the $^{\bullet}O_2^-$ free radical could be on protonation yields the HOO• radical and finally formed •OH radical [44]. The photogenerated h^+ transferred to the AgCl surface to oxidate the Cl^- to Cl° atoms. The Cl° atoms were reactive radical species to oxidize dye molecules and hence reduced to Cl^- again. (Fig. S4, Supporting information) Interesting, in the Ag/AgCl/$NaTaO_3$ system, the mechanism was

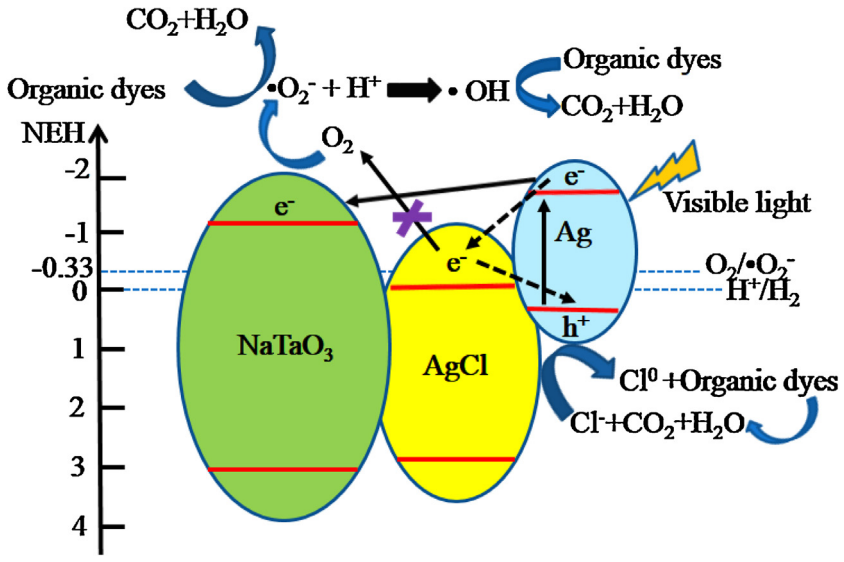

Fig. 12. Schematic diagram for the charge separation in a visible light irradiated Ag/AgCl/$NaTaO_3$ system.

shown in Fig. 12, the metallic Ag NPs absorb the visible light to produce electron-hole pairs. The photoexcited e^- from the Ag NPs are injected into the conduction band of $NaTaO_3$ and AgCl. Then the e^- on the surface of $NaTaO_3$ transfer to the molecular oxygen to form $^{\bullet}O_2^-$ free radical because the conduction band of $NaTaO_3$ is lower than the E_0 ($O_2/^{\bullet}O_2^-$) (−0.33 eV vs NHE). This electron transfer process can decrease the recombination of charges. However, the photoexcited e^- on the surface of AgCl could not transfer to the O_2 to form $^{\bullet}O^{2-}$ free radical because the conduction band of AgCl is lower than the E_0 ($O_2/^{\bullet}O^{2-}$) (−0.33 eV vs NHE). Therefore, the e^- recombine with the h^+ inside of Ag NPs (as the dotted line shown). From the active species trapping experiment and ESR results, it conclude that most part of the $^{\bullet}O_2^-$ free radical on the surface of $NaTaO_3$ can degrade the dyes molecules. But a little part of the $^{\bullet}O_2^-$ form $^{\bullet}OH$ radical to degrade the dyes. The h^+ of Ag NPs transfer to the AgCl surface are most react with Cl^- to Cl° atoms [45–48]. Moreover, the Cl° atoms are reactive species which are able to oxidize dyes molecules and become reduced to Cl^- again so that the Ag/AgCl/$NaTaO_3$ system remains stable [49,50]. In the summary, Ag/AgCl NPs loaded on the surface of $NaTaO_3$ nanocubes have formed plasmonic Ag/AgCl/$NaTaO_3$ photocatalysts enhancing the photocatalytic activity for degrading organic dyes.

4. Conclusions

In summary, the plasmonic photocatalyst Ag/AgCl/$NaTaO_3$ nanocubes were successfully synthesized through precipitation and photoreduction methods. The as-prepared samples were characterized by XRD, SEM, TEM, EDS and XPS measurements. With the present synthetic strategy, the Ag/AgCl/$NaTaO_3$ composites showed higher photocatalytic activity for the organic dyes degradation of RhB and MB under visible light irradiation then the pure $NaTaO_3$ and Ag/AgCl particles. In addition, the photocatalyst exhibited high stability and photocatalytic activity with almost no loss after five cycles of photocatalytic reaction. The enhanced photocatalytic performance can be mainly attributed to the SPR with strong visible light absorbance and efficient charge separation on the surface. In general, the plasmonic Ag/AgCl/$NaTaO_3$ composites photocatalyst with the strong visible light absorption and efficient photocatalytic activity and stability, have been extended application in photocatalysis for organic dyes pollutants degradation and purification of water.

Acknowledgments

The authors would like to acknowledge the National Natural Science Foundation of China (21276116, 21477050, 21301076, 21303074, 21401082, 21522603 and 21576121), the Chinese-German Cooperation Research Project (GZ1091), the Excellent Youth Foundation of Jiangsu Scientific Committee (BK20140011), the Program for New Century Excellent Talents in University (NCET-13-0835), the Henry Fok Education Foundation (141068) and Six Talents Peak Project in Jiangsu Province (XCL-025).

Appendix A. Supplementary data

Supplementary data associated with this article can be found, in the online version, at http://dx.doi.org/10.1016/j.apcatb.2016.03.036.

References

[1] Z. Aksu, Process Biochem. 40 (2005) 997–1026.
[2] A. Kudo, Y. Miseki, Chem. Soc. Rev. 38 (2009) 253–278.
[3] M.R. Hoffmann, S.T. Martin, W.Y. Choi, D.W. Bahnemann, Chem. Rev. 95 (1995) 69–96.
[4] J.L. Zhang, Y.M. Wu, M.Y. Xing, S.A. Leghari, K.S. Sajjad, Energy Environ. Sci. 3 (2010) 715–726.
[5] K.F. Li, X.Q. An, K.H. Park, M. Khraisheh, J.W. Tang, Catal. Today 224 (2014) 3–12.
[6] P. Wang, B.B. Huang, Y. Dai, M.H. Whangbo, Phys. Chem. Chem. Phys. 14 (2012) 9813–9825.
[7] Z. Liu, Z.G. Zhao, M. Miyauchi, J. Phys. Chem. C 113 (2009) 17132–17137.
[8] Y.G. Xu, H. Xu, J. Yan, H.M. Li, L.Y. Huang, Q. Zhang, C.J. Huang, H.L. Wan, Phys. Chem. Chem. Phys. 15 (2013) 5821–5830.
[9] L. Sun, R.Z. Zhang, Y. Wang, W. Chen, ACS Appl. Mater. Interfaces 6 (2014) 14819–14826.
[10] S.N. Alamdari, A.H. Yangjeh, M. Pirhashemi, Solid State Sci. 40 (2015) 111–120.
[11] P. Wang, B.B. Huang, Q.Q. Zhang, X.Y. Zhang, X.Y. Qin, Y. Dai, J. Zhan, J.X. Yu, H.X. Liu, Z.Z. Lou, Chem. Eur. J. 16 (2010) 10042–10047.
[12] Y.Y. Li, Y. Ding, J. Phys. Chem. C 114 (2010) 3175–3179.
[13] C. Hu, T. Peng, X. Hu, Y.L. Nie, X.F. Zhou, J.H. Qu, H. He, J. Am. Chem. Soc. 132 (2009) 857–862.
[14] Z.Z. Lou, B.B. Huang, P. Wang, Z.Y. Wang, X.Y. Qin, X.Y. Zhang, H.F. Cheng, Z.K. Zheng, Y. Dai, Dalton Trans. 40 (2011) 4104–4110.
[15] C.C. Jia, P. Yang, B.B. Huang, ChemCatChem 6 (2014) 611–617.
[16] Y. Hosogi, Y. Shimodaria, H. Kato, H. Kabayashi, A. Kudo, Chem. Mater. 20 (2008) 1299–1307.
[17] T.G. Xu, X. Zhao, Y.F. Zhu, J. Phys. Chem. B 110 (2006) 25825–25832.
[18] H. Kato, A. Kudo, J. Phys. Chem. B 105 (2001) 4285–4292.
[19] H. Kato, A. Kudo, J. Am. Chem. Soc. 125 (2003) 3082–3089.
[20] H. Kato, A. Kudo, Catal. Today 78 (2003) 561–569.
[21] X. Li, J.L. Zang, J. Phys. Chem. C 113 (2009) 19411–19418.
[22] L.H. Ai, C.H. Zhang, J. Jiang, Appl. Catal. B 142 (2013) 744–751.
[23] P. Wang, B.B. Huang, Z.Z. Lou, X.Y. Zhang, X.Y. Qin, Y. Dai, Z.K. Zheng, X.N. Wang, Chem. Eur. J. 16 (2010) 538–544.
[24] R.F. Dong, B.Z. Tian, C.Y. Zeng, T.Y. Li, T.T. Wang, J.L. Zhang, J. Phys. Chem. C 117 (2013) 213–220.
[25] L. Sun, R.Z. Zhang, Y. Wang, W. Chen, ACS Appl. Mater. Interfaces 6 (2014) 14819–14826.
[26] Y.H. Liang, S.L. Lin, L. Liu, J.S. Hu, W.Q. Cui, Appl. Catal. B 164 (2015) 192–203.
[27] H. Zhang, G. Wang, D. Chen, X.J. Lv, J.H. Li, Chem. Mater. 20 (2008) 6543–6549.
[28] L.H. Dong, D.D. Liang, R.C. Gong, Eur. J. Inorg. Chem. 19 (2012) 3200–3208.
[29] D.B. Xu, M. Chen, S.Y. Song, D.L. Jiang, W.Q. Fan, W.D. Shi, CrystEngComm 16 (2014) 1384–1388.
[30] D.B. Xu, K.L. Liu, W.D. Shi, M. Chen, B.F. Luo, L.S. Xiao, W. Gu, Ceram. Int. 41 (2015) 4444–4451.
[31] P. Wang, B.B. Huang, X.Y. Zhang, X.Y. Qin, H. Jin, Y. Dai, Z.Y. Wang, J.Y. Wei, J. Zhan, S.Y. Wang, J.P. Wang, M.H. Whangbo, Chem. Eur. J. 15 (2009) 12576–12579.
[32] G.T. Li, K.H. Wong, X.W. Zhang, C. Hu, J.C. Yu, R.C.Y. Chan, P.K. Wong, Chemosphere 76 (2009) 1185–1196.
[33] D.B. Xu, S.B. Yang, Y. Jin, M. Chen, W.Q. Fan, B.F. Luo, W.D. Shi, Langmuir 31 (2015) 9694–9699.
[34] X. Liang, H. Tao, Q. Zhang, C.T. Chang, J. Nanosci. Nanotechnol. 15 (2015) 4887–4894.
[35] J. Cao, B.Y. Xu, H.L. Lin, B.D. Luo, S.F. Chen, Chem. Eng. J. 185 (2012) 91–100.
[36] Z.J. Zhou, M.C. Long, W.M. Cai, J. Cai, J. Mol. Catal. A: Chem. 353 (2012) 22–28.
[37] Q. Xiao, Z.C. Si, J. Zhang, C. Xiao, X.K. Tan, J. Hazard. Mater. 150 (2008) 62–67.
[38] L.S. Zhang, K.H. Wong, H.Y. Yip, C. Hu, J.M. Yu, C.Y. Chan, P.K. Wong, Environ. Sci. Technol. 44 (2010) 1392–1398.
[39] J.Q. Yan, G.J. Wu, N.J. Guan, L.D. Li, Chem. Commun. 49 (2013) 11767–11769.
[40] J. Jiang, X. Zhang, P.B. Sun, L.Z. Zhang, J. Phys. Chem. C 115 (2011) 20555–20564.
[41] Q.J. Xiang, J.G. Yu, M.J. Jaroniec, Phys. Chem. C 115 (2011) 7355–7363.
[42] P. Wang, B.B. Huang, X.Y. Qin, X.Y. Zhang, Y. Dai, J.Y. Wei, M.H. Whangbo, Angew. Chem. Int. Ed. 47 (2008) 7931–7933.
[43] Y. Tian, T. Tatsuma, J. Am. Chem. Soc. 127 (2005) 7632–7637.
[44] T.X. Wu, G.M. Liu, J.C. Zhao, H. Hidaka, N. Serpone, J. Phys. Chem. B 102 (1998) 5845–5851.
[45] Y. Xu, H. Xu, H. Li, J. Xia, C. Liu, L. Liu, J. Alloys Compd. 509 (2011) 3286–3292.
[46] G. Begum, J. Manna, R.K. Rana, Chem. Eur. J. 18 (2012) 6847–6853.
[47] F. Chen, H. Liu, S. Bagwasi, X. Shen, J.J. Zhang, Photochem. Photobiol. A 215 (2010) 76–80.
[48] M.A. Gondal, X.F. Chang, Z.H. Yamani, Chem. Eng. J. 165 (2010) 250–257.
[49] H.J. Yan, S.J.T. Kochuveedu, L.N. Quan, S.S. Lee, D.H. Kim, J. Alloys Compd. 560 (2013) 20–26.
[50] R.F. Dong, B.Z. Tian, C.Y. Zeng, T.Y. Li, T.T. Wang, J.L.J. Zhang, J. Phys. Chem. C 117 (2013) 213–220.